

---

---

OPTICS OF LOW-DIMENSIONAL STRUCTURES,  
MESOSTRUCTURES, AND METAMATERIALS

---

---

## The Role of Physical Models in the Description of Luminescence Kinetics of Hybrid Nanowires

A. S. Kulagina<sup>a,\*</sup>, A. I. Khrebtov<sup>a</sup>, R. R. Reznik<sup>b</sup>, E. V. Ubyivovk<sup>b,c</sup>, A. P. Litvin<sup>b</sup>, I. D. Skurlov<sup>b</sup>,  
G. E. Cirilin<sup>a,b,d,e</sup>, E. N. Bodunov<sup>f</sup>, and V. V. Danilov<sup>f</sup>

<sup>a</sup> Alferov University, Russian Academy of Sciences, St. Petersburg, 194021 Russia

<sup>b</sup> ITMO University, St. Petersburg, 197101 Russia

<sup>c</sup> St. Petersburg University, St. Petersburg, 199034 Russia

<sup>d</sup> Institute for Analytical Instrumentation of the Russian Academy of Sciences, St. Petersburg, 190103 Russia

<sup>e</sup> Saint Petersburg Electrotechnical University, St. Petersburg, 197376 Russia

<sup>f</sup> Emperor Alexander I St. Petersburg State Transport University, St. Petersburg, 191031 Russia

\*e-mail: a.s.panfutova@gmail.com

Received September 9, 2019; revised September 9, 2019; accepted September 26, 2019

**Abstract**—The luminescence photodynamics of an array of InP/InAsP/InP nanowires formed via molecular beam epitaxy onto a Si(III) substrate is investigated in this work. Using several kinetic models, the experimental data acquired by a 633-nm room-temperature laser excitation have been analyzed. The kinetics of luminescence decay of the InAsP nanoinset is shown to be best described in the context of the model of contact quenching. The total time of decay of the excited state (the radiative lifetime) of the InAsP nanoinset is estimated to be  $\tau \sim 40$  ns. The reasons of unexpectedly long duration of the excitation transfer from InP are discussed as well.

**Keywords:** hybrid nanowires, kinetics of luminescence, photodynamics

**DOI:** 10.1134/S0030400X20010129

### INTRODUCTION

Currently, semiconducting nanowires (NWs) are finding application in many fields of photovoltaics, photodetection, optoelectronics, medicine, and other areas due to their unique properties [1–4]. Special attention is paid to the ability of creating nanoinset-like heterostructures (or quantum dots) in an NW body with a large bandgap, which allows one to expand the emission range of NWs, as well as to obtain singular-photon sources and to form directed radiation sources [5–8]. Meanwhile, semiconducting nanocrystals are often characterized by a complex dynamic of excited state. This explains the need for understanding the physical principles that tune the luminescence photodynamics in nanostructures. From this viewpoint, spectrokinetic methods seem to be the most informative [9–12]. However, the lack of stable formalism leads to ambiguities in the interpretation of experimental data. In that case, the quality of luminescence kinetic data processing becomes essential [13–17]. The present work is aimed at investigating the photoluminescence (PL) kinetics of a hybrid semiconducting nanostructure, namely an InP/InAsP/InP NW array formed via molecular beam epitaxy onto a Si(III) substrate, using several physical models for

approximation of experimental kinetic data. A comparative analysis of results enabled us to thoroughly describe the luminescence photodynamics of this structure.

### EXPERIMENTAL

NWs were synthesized via molecular beam epitaxy using a Compact21 setup (Riber). The average height of InP NWs was 4  $\mu\text{m}$ , and the diameter was irregular over height, being 100 nm at the base and 30 nm at the top of the NWs at a surface density of  $3 \times 10^8 \text{ cm}^{-2}$ . The InAsP nanoinset (NI) (with an As content of  $\sim 40\%$ ) was 60 nm-long and 5-nm-large (Fig. 1a) (the NI occurrence depth in the NWs was  $\sim 10$  nm).

Figure 1a shows the radial trace of the same material at some distance from InAsP NI. It is a radial quantum well (QW) with the average arsenic content of 15–25%, formed in the course of deposition of a thin InAsP layer onto the InP surface during the formation of NIs.

Figure 1b displays the luminescence spectrum of the grown structure, excited by a continuously emitting laser at a wavelength of 633 nm at a radiation power of about 6 mW. The secondary radiation was

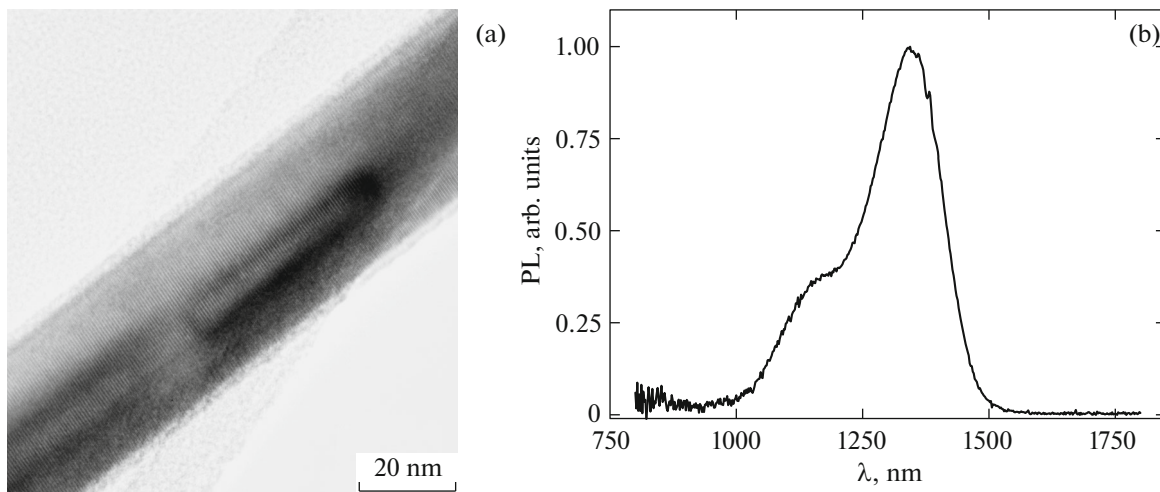


**Fig. 1.** (a) TEM image of the InAs NW area with InAsP NI; (b) PL spectrum of the InP NW array with NI InAsP.

collected in conformity with the standard scheme at an angle of  $90^\circ$ , and the exciting radiation was rejected by a KS19 light filter (the cutoff wavelength was 680 nm). The spectra were normalized to the detector sensitivity.

The PL spectra and kinetics were measured from a NW array with an area of about  $5 \mu\text{m}^2$  and were recorded in the near-IR range by an InGaAs photodiode (Hamamatsu).

The luminescence kinetics was studied using a pulsed laser with a wavelength of 633 nm (repetition rate of  $\sim 2.5$  MHz, pulse energy of  $\sim 6$  nJ, and pulse duration of  $< 100$  ps) as the excitation source. The luminescence kinetic curves for the NI were recorded at a wavelength of 1350 nm. All the measurements were taken at room temperature ( $T = 293$  K).

## RESULTS AND DISCUSSION

As can be seen in Fig. 1b, the luminescence spectra of InAsP/InP NW arrays exhibit high-intensity bands at 1.0–1.5  $\mu\text{m}$ . The luminescence band at 1.25–1.5  $\mu\text{m}$  corresponds to the glow of the InAsP NI. A short-wave band at 1.0–1.2  $\mu\text{m}$  is attributed to the glow of a radial QW. At a fixed excitation geometry, the observed band intensity redistribution is due to the different absorption spectra of the NI and QW.

The room-temperature luminescence decay of nanocrystals often behaves as a nonexponential function [18–20], which can be written as a sum of several exponents:

$$I_{\text{norm}} = \sum_i A_i e^{-t/\tau_i}.$$

Here,  $I_{\text{norm}}$  is the luminescence decay intensity normalized per unit at the initial moment of time; the condition applied to the amplitudes is  $\sum A_i = 1$ . Such

an approach implies the existence of either various nonradiatively coupled metastable states or diverse groups of nanocrystals with different morphology and different luminescence decay times. The relative amount of these states (or groups) in the total decay kinetics is characterized by coefficients  $A_i$  at the exponents. (A similar situation occurs in triplet–triplet annihilation [21, 22].)

As can be seen from Fig. 2, the luminescence decay kinetics curves of InAsP NI at room-temperature and nitrogen temperature are very close. Thus, a further analysis will be performed for only a case of 293 K. The best approximation of experimental data is achieved by using the decay function as a sum of two exponents:

$$I_{\text{norm}} = A_1 e^{-t/\tau_1} + A_2 e^{-t/\tau_2}, \quad (1)$$

where  $A_1 + A_2 = 1$ . The approximation parameters are given in Table 1.

The decay time range, which is shown in Table 1, was determined from a series of identical experiments and is due to the differences in geometry and morphology of NWs in the array. As can be seen, the luminescence decay from the ground excited state of the NI (remains undistinguished in the spectrum) represents a sum of two components with decay times of 10 and 45 ns. Thus, the amplitude of the first compo-

**Table 1.** Luminescence lifetimes of NI and their amplitudes for model (1)

Parameters of model (1)	Values
$A_1$	0.66
$\tau_1$ , ns	5–8
$A_2$	0.34
$\tau_2$ , ns	25–44

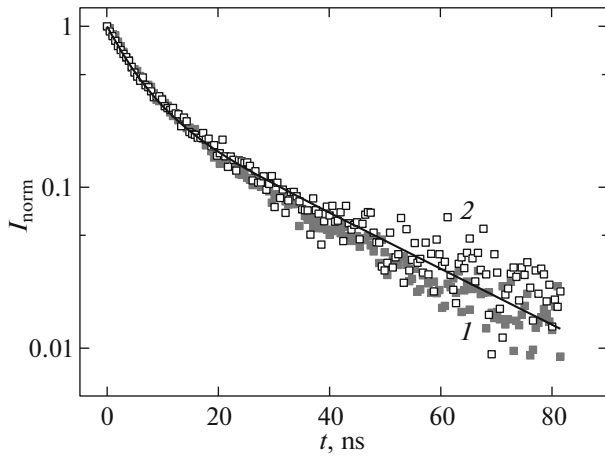


**Fig. 2.** Normalized experimental luminescence kinetics of the NI (points), measured at (1) 77 and (2) 293 K and its approximation using function (1) (solid curve).

ment ( $A_1$ ) is twice as large as the amplitude of the second one ( $A_2$ ). One can, thus, assume that the luminescence of the NI (besides the direct excitation) has an additional excitation state pump channel from traps or on as a result of any excitation transfer from the QW and the InP array.

In order to establish the influence of QW on the kinetics of NI, a series of measurements of luminescence kinetics of QWs was performed. The kinetics of QWs was recorded at a wavelength of 1145 nm and was best described by one exponent. As found, the luminescence lifetime for QWs was smaller than 10 ns, which coincides with the decay time of the short component of the NI. Since the emitting centers of QW and NI are almost identical, the lifetimes of their radiative states should be close to each other. A comparative analysis of luminescence decay kinetic curves for NI and QW enabled us to associate the short luminescence component of the NI (with  $t_1$  on the order of 10 ns) with the decay time of the excited state of the InAsP NI. Hence, taking into account the quantum yield for our system determined from the luminescence amplitude as a function of the excitation power [23] ( $\sim 0.4$ – $0.5$  [8]), the natural lifetime of the excited state for the NI is estimated to be  $\sim 10$ – $20$  ns.

The long decay component has a complex nature. On the one hand, it can be determined by the excited state of InP, which populates the emitting state of NI via the radiative and nonradiative excitation transfers. Thus, the lifetime of NI InAsP as a function of diameter ( $d$ ) of InP NWs was established in work [24], allowing the ratio of  $d/\lambda$ , where  $\lambda$  is the luminescence wavelength of NI. For our samples, this ratio has a value of 0.022 and, according to the experimental dependence given in work [24], the radiation lifetime must exceed 25 ns. Meanwhile, the excitation photo-dynamics of InAsP through this channel, although

being partly explained by the authors [24], requires further clarification. On the other hand, an increase in the radiative recombination duration of InAsP in InP NWs may be due to a spatial separation of charge carriers in NI because of a second-order heteroboundary between NI InAsP and InP NWs [25, 26]. A similar effect was observed in GaAs/AlGaAs NWs and was interpreted by the emergence of domains with various crystal lattice types in NWs [27].

In works [14, 15], the luminescence decay kinetics of colloidal solutions of CdSe/ZnS quantum dots was proposed to be interpreted using a stretched exponential function [20]:

$$I_{\text{norm}}(t) = \exp\left[-\frac{t}{\tau} - a\left(\frac{t}{\tau}\right)^\beta\right]. \quad (2)$$

Here,  $\tau$  is the lifetime of the excited state of luminescent quantum dots, parameter  $\beta$  has values in the range of  $0 < \beta \leq 1$  and depends on the luminescence quenching mechanisms (dipole–dipole, dipole–quadrupole, or quadrupole–quadrupole), and  $a$  is a constant that depends on the concentration of quenching molecules. The fitting parameters in Eq. (2) are coefficients  $\tau$ ,  $a$ , and  $\beta$ . It should be noted that the time  $\tau$  can be determined from the independent experiments. The number of fitting parameters is then reduced to two. It is worth noting that this approach in the case of luminescence allows one to ground the principle of invariability of the natural lifetime of the unique radiative state [28]. Unlike the radiation lifetime, the natural lifetime is independent of the temperature, which also entails a room-temperature description of luminescence. At fixed parameter  $\tau$ , values  $\beta$  in the kinetics can be associated with luminescence decay processes of different nature. Function (2) is often used for the description of luminescence decay kinetics at a Forster resonant energy transfer (FRET) from the energy-donor molecules to the acceptor molecules. This function was then used to describe the luminescence kinetics of samples.

It follows from the results (Fig. 3) that the decay time of the radiative state is  $\sim 45$  ns, which is close to the total duration of the two components from Table 1. Furthermore, a satisfactory description of experimental data using this model at  $\beta = 0.5$  reveals that the main mechanism of luminescence extinction of NI is the dipole–dipole energy transfer to the extincors [15, 29].

As was discussed above, the light irradiation excites not only the NI, but also the QW. Since the luminescence spectrum of the QW is shifted to the short-wave range of the luminescence spectrum of the NI, in addition to pronounced radiative transfer, there may also be nonradiative energy transfer (FRET) from the QW to the NI. Thus, the NI can be excited by both the direct excitation and the FRET (sensitized luminescence). Solving the relevant kinetic equations (a three-level system, i.e., the excited state of the QW and the

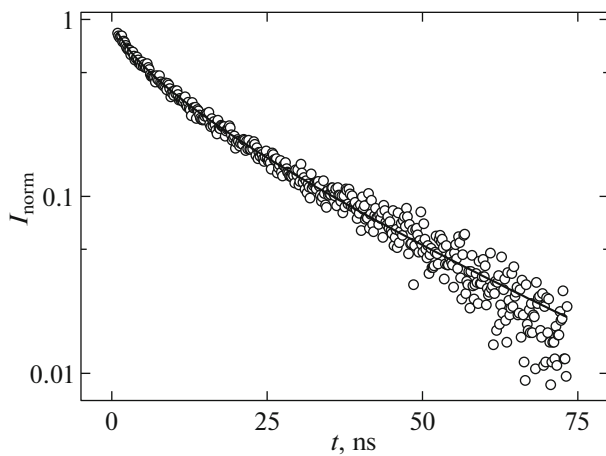


**Fig. 3.** Normalized experimental luminescence kinetic curve of the NI (points) and its approximation using function (2) (solid curve) at  $\tau = 45$  ns,  $\beta = 0.5$  and  $a = 1.8$ .

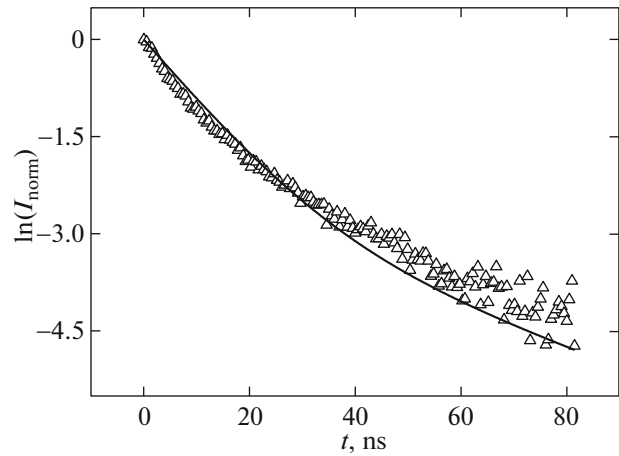


**Fig. 4.** Normalized experimental luminescence kinetic curve of the NI (points) in the logarithmic scale and its approximation using function (3) (solid curve).

excited and the ground states of the NI) yields the following formula for the luminescence decay kinetics of the NI, given the additional excitation through the QW:

$$I_{\text{norm}}(t) = e^{-t/\tau} \left[ 1 + \frac{kB}{1/\tau_{\text{QW}} - 1/\tau + k} (1 - e^{-(1/\tau_{\text{QW}} - 1/\tau + k)t}) \right], \quad (3)$$

where  $\tau_{\text{QW}}$  is the luminescence decay time of the QW,  $\tau$  is the lifetime of the excited state of the NI,  $k$  is the rate of the energy transfer from the QW to the NI, and  $B$  is the parameter characterizing the degree of excitation of the QW at the initial moment of time. The fitting parameters in this model are  $\tau_{\text{QW}}$ ,  $\tau$ ,  $k$ , and  $B$ . As can be seen in Fig. 4, the luminescence decay kinetics of the NI is unsatisfactorily described by function (3).

This result is interpreted in terms of the absence of FRET, which is because of the large distance between the NI and the QW. Below, Table 2 shows the approximation parameters corresponding to Fig. 4.

The radiative lifetime of a quantum well, the value of which was found to be 100 ns within the framework of this model, is, however, uncertain. We assume that, although the nonradiative energy transfer from the

QW to the NI undeniably exists and is determined by the overlap of the luminescence spectrum of the QW and the absorption spectrum of the NI, the luminescence decay kinetics will depend on the lifetime of the emitting state of the NI. As we have already established, the lifetimes of the emitting states of InAsP and NI InAsP QWs are close to each other. In this case, the contribution from the QW to the luminescence spectrum of the NI has almost no effect on the luminescence kinetics of the NI. To explain the value  $\tau_{\text{QW}} = 100$  ns obtained using model (3), one can assume the existence of the long-term metastable states that are described in works [13, 30, 31]. These states are not seen at the initial stages of the luminescence kinetics of the QW, but begin to manifest themselves in the approximation of the kinetic distribution “tails.”

In addition to the FRET, the luminescence decay kinetics is often described via the model of “contact quenching” [15, 32]. This model is based on the following assumptions. The energy acceptors (charge carrier traps) are located at the surface of the quantum dots (the distance between the donor and the acceptor is less than 1 nm). The trap distribution over the quantum dots obeys a Poisson law, like molecule distribution on micelle surface [33]. It is worth mentioning that charge carrier traps are always present in semiconducting nanocrystals. They exert fundamental influence on the excited state relaxation, which makes important their nature and role in photodynamics of the whole nanostructure. Bulk structural deformations at the interface of crystal lattices (in our case, InP and InAsP) are known to be another reason for the emergence of traps [26, 27]. In this model, the contact luminescence kinetics rate  $k$  of the NI by one acceptor is assumed similar for all traps. The average number of traps near the NI is  $N_{\text{av}}$ ,  $\tau$  is the radiative recombination time of the NI. Given these assumptions, the

**Table 2.** Luminescence lifetimes of NI and QW in conformity with model (3)

Parameters of model (3)	Values
$\tau_{\text{QW}}$ , ns	100
$\tau$ , ns	10
$k$ , ns <sup>-1</sup>	0.02
$B$	0.325

\* at fixed parameter  $\tau$ .

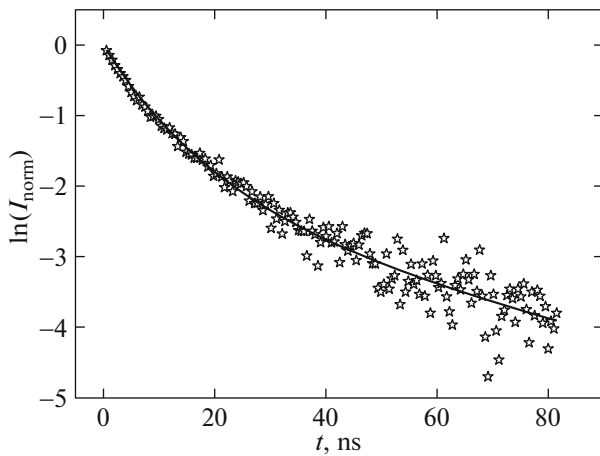


**Fig. 5.** Normalized experimental luminescence kinetic curve of the NI (points) and its approximation using function (4) (solid curve) at  $\tau = 40$  ns,  $N_{av} = 2$  and  $k = 1.9$  ns $^{-1}$ .

function describing the luminescence kinetics in obedience to the contact mechanism is written as follows:

$$I_{\text{norm}}(t) = \exp\left(-\frac{t}{\tau} - N_{av}\left(1 - \exp\left(-k\frac{t}{\tau}\right)\right)\right). \quad (4)$$

Here, the fitting parameters are  $\tau$ ,  $k$ , and  $N_{av}$ .

As can be seen in Fig. 5, the luminescence decay kinetics of the NI is well described via the model of “contact quenching” (function (4)). Note that the time  $\tau$  coincides with a value calculated using the model (2). Since the experimental kinetics curves are adequately described by function (4), there is no need to take the excitation return from the traps to the NI into account. It is clear that the return rate is negligibly small and considering it requires going beyond the measurement accuracy.

Thus, we assume that contact quenching is the dominating mechanism in the relaxation kinetics of the excited state of the NI. In other words, the defects existing at the interface between the NI and the InP array are the main reason of the luminescence quenching of the NI.

## CONCLUSIONS

The efficiency of parallel processing of the spectral kinetic dependences using various functions was shown by the example of an InP NW/ InAsP NI artificial structure. The natural luminescence lifetime of the InAsP NI was found to be about 10 ns for a given structure. The role of the QW (similar with a chemical composition of the NI) and the InP NW array in the population of the excited state of NI, as well as possible mechanisms of luminescence quenching of the NI, were discussed. The analysis of luminescence decay kinetics reveals that the quenching kinetics of the NI is best described in the context of the model of contact quenching, and the total decay time of the excited state

(radiative lifetime) is estimated to be on the order of magnitude of 40 ns. The reasons of the unexpectedly large time of excitation transfer from InP to NI were discussed as well.

## FUNDING

This work was supported by the Ministry of Science and Higher Education of the Russian Federation, state order no. 16.9791.2017/8.9. The samples were grown with the financial support of the Russian Science Foundation, project no. 19-72-30010.

## CONFLICT OF INTEREST

The authors declare that they have no conflict of interest.

## REFERENCES

1. R. R. LaPierre, A. C. E. Chia, S. J. Gibson, C. M. Haapamaki, J. Boulanger, R. Yee, P. Kuyanov, J. Zhang, N. Tajik, N. Jewell, and K. M. A. Rahman, *Phys. Status Solidi RRL* **7**, 815 (2013).
2. R. Yan, D. Gargas, and P. Yang, *Nat. Photon.* **3**, 569 (2009).
3. Y. Zhang, J. Wu, M. Aagesen, and H. Liu, *J. Phys. D: Appl. Phys.* **48**, 463001 (2015).
4. F. Patolsky, G. Zheng, and C. M. Lieber, *Nanomedicine* **1**, 51 (2006).
5. G. E. Cirlin, I. V. Shtrom, R. R. Reznik, Y. B. Samsonenko, A. I. Khrebtov, A. D. Bouravleuv, and I. P. Soshnikov, *Semiconductors* **50**, 1421 (2016).
6. P. Kuyanov and R. R. LaPierre, *Nanotechnology* **26**, 315202 (2015).
7. A. I. Khrebtov, R. R. Reznik, E. V. Ubyivovk, A. P. Litvin, I. D. Skurlov, P. S. Parfenov, A. S. Kulagina, V. V. Danilov, and G. E. Cirlin, *Semiconductors* **53**, 1258 (2019).
8. M. E. Reimer, G. Bulgarini, N. Akopian, M. Hocevar, M. B. Bavinck, M. A. Verheijen, E. P. A. M. Bakkers, L. P. Kouwenhoven, and V. Zwiller, *Nat. Commun.* **3** (737) (2012).  
<https://doi.org/10.1038/ncomms1746>
9. J. M. Pietryga, Y-S. Park, J. Lim, A. F. Fidler, W. K. Bae, S. Browelli, and V. I. Klimov, *Chem. Rev.* **116**, 10513 (2016).
10. V. V. Danilov, A. S. Panfutova, G. M. Ermolaeva, A. I. Khrebtov, and V. B. Shilov, *Opt. Spectrosc.* **114**, 880 (2013).
11. D. Spirkoska, G. Abstreiter, and A. Fontcuberta i Morral, *Nanotechnology* **19**, 435704 (2008).
12. M. S. Smirnov, O. V. Ovchinnikov, and A. S. Perepelitsa, *Opt. Spectrosc.* **126**, 62 (2019).
13. E. N. Bodunov and A. L. Simões Gamboa, *J. Phys. Chem. C* **123**, 25515 (2018).  
<https://doi.org/10.1021/acs.jpcc.9b07619>
14. E. N. Bodunov, V. V. Danilov, A. S. Panfutova, and A. L. Simões Gamboa, *Ann. Phys. (Berlin)* **528**, 272 (2016).  
<https://doi.org/10.1002/andp.201500350>

15. E. N. Bodunov, Y. A. Antonov, and A. L. Simões Gamboa, *J. Chem. Phys.* **146**, 114102 (2017).  
<https://doi.org/10.1063/1.4978396>
16. L. Brus, *Phys. Rev. B* **53**, 4649 (1996).
17. S. Chen, M. Yoshita, A. Ishikawa, T. Mochizuki, S. Maruyama, H. Akiyama, Y. Hayamizu, L. N. Pfeiffer, and K. W. West, *Sci. Rep.* **3**, 1941 (2013).  
<https://doi.org/10.1038/srep01941>
18. T. D. Krauss and J. J. Peterson, *Nat. Mater* **11**, 14 (2012).
19. C. de Mello Donegá, M. Bode, and A. Meijerink, *Phys. Rev. B* **74**, 085320 (2006).
20. M. N. Berberan-Santos, E. N. Bodunov, and B. Valeur, *Chem. Phys.* **315**, 171 (2005).  
<https://doi.org/10.1016/j.chemphys.2005.04.006>
21. E. N. Bodunov, M. N. Berberan-Santos, and J. M. G. Martinho, *Chem. Phys.* **316**, 217 (2005).  
<https://doi.org/10.1016/j.chemphys.2005.05.020>
22. M. N. Berberan-Santos, E. N. Bodunov, and J. M. G. Martinho, *Opt. Spectrosc.* **99**, 918 (2005).  
<https://doi.org/10.1134/1.2149416>
23. Y. -S. Park, A. V. Malko, J. Vela, Y. Chen, Y. Ghosh, F. Garcia-Santamaria, J. A. Hollingsworth, V. I. Klimov, and H. Htoon, *Phys. Rev. Lett.* **106**, 187401 (2011).
24. G. Bulgarini, M. E. Reimer, T. Zehender, M. Hocevar, E. Bakkers, L. P. Kouwenhoven, and V. Zwiller, *Appl. Phys. Lett.* **100**, 121106 (2012).
25. L. V. Asryan and S. Luryi, *IEEE J. Quantum Electron.* **37**, 905 (2001).
26. B. Pal, K. Goto, M. Ikezawa, Y. Masumoto, P. Mohan, J. Motohisa, and T. Fukui, *Appl. Phys. Lett.* **93**, 073105 (2008).
27. V. G. Talalaev, A. V. Senichev, B. V. Novikov, J. W. Tomm, T. Elsaesser, N. D. Zakharov, P. Werner, U. Gösele, Y. B. Samsonenko, and G. E. Cirlin, *Semiconductors* **44**, 1050 (2010).
28. P. A. M. Dirac, *The Principles of Quantum Mechanics* (Oxford Univ. Press, Oxford, 1930).
29. V. L. Ermolaev, E. N. Bodunov, E. B. Sveshnikova, and T. A. Shakhverdov, *Nonradiative Transfer of Electronic Excitation Energy* (Nauka, Leningrad, 1977) [in Russian].
30. E. N. Bodunov and A. L. Simões Gamboa, *J. Phys. Chem. C* **122**, 10637 (2018).  
<https://doi.org/10.1021/acs.jpcc.8b02779>
31. E. N. Bodunov and A. L. Simões Gamboa, *Semiconductors* **53**, 2133 (2019).  
<https://doi.org/10.1134/S1063782619120078>
32. E. N. Bodunov and A. L. Simões Gamboa, *Semiconductors* **52**, 587 (2018).  
<https://doi.org/10.1134/S1063782618050044>
33. E. N. Bodunov, M. N. Berberan-Santos, and J. M. G. Martinho, *Chem. Phys. Lett.* **297**, 419 (1998).  
[https://doi.org/10.1016/S0009-2614\(98\)01151-8](https://doi.org/10.1016/S0009-2614(98)01151-8)

*Translated by O. Maslova*